Nanoporous Films

Synthesis of a Large-Scale Highly Ordered Porous Carbon Film by Self-Assembly of Block Copolymers**

*Chengdu Liang, Kunlun Hong, Georges A. Guiochon, Jimmy W. Mays, and Sheng Dai**

Elemental carbon materials exhibit unique electronic, mechanical, and chemical properties that make them attractive, for example, for nanoelectronic devices,[1] strength-enhancing materials,[2] separation media,[3–6] catalyst supports,[7] energy storage/conversion systems,[8] proximal probes,[9] optical components.[10] Well-defined nanoporous carbon materials are essential for a number of these applications. Ordered porous carbon materials have previously been replicated by using colloidal crystals[10] and presynthesized mesoporous silicas as scaffolds.[7] These methodologies are extremely difficult to adapt to the fabrication of large-scale ordered nanoporous films with controlled pore orientations. Although numerous methods (e.g., chemical vapor deposition,[11] ultrasonic deposition,[3a] silica template synthesis,[3b,7] hydrothermal decomposition of carbide compounds,[12] and polymer coating and pyrolysis[13]) have been developed for the fabrication of carbon films, no ordered nanoporous carbon films have been obtained with such methods. Accordingly, the large-scale alignment of the carbon nanostructural films is still a big challenge. Herein, we demonstrate a stepwise self-assembly approach to the preparation of large-scale, highly ordered nanoporous carbon films. The carbon precursor molecules are spatially arranged into well-defined nanostructures by the self-assembly of block copolymers (BCPs). A hexagonally packed carbon-channel array whose orientation is normal to the carbon film surface has been successfully synthesized. Large-scale crack-free carbon films of up to 6 cm^2 can be readily fabricated on common substrates such as silica, copper, silicon, and carbon.

The self-assembly of BCPs has proven to be a versatile approach to the selective organization and nanoscale regulation of the concentration distribution of target molecular species for the fabrication of nanoporous materials.[14–16] The mechanism for such organization involves hydrogen-bonding,[17] ion-pairing,[18] and/or dative interactions[19] between supramolecular assemblies of BCPs and target molecular species. The resulting composites can give rise to various nanostructures according to the structural and phase behaviors of the BCPs. The target molecular species are spatially concentrated in selected microdomains and can eventually serve as nanostructured catalysts,[20] spacers,[21] or precursors[22] for the further fabrication of ordered nanostructures. Highly ordered nanoporous materials, such as polymer,[22] silica,[23,24] and organic–inorganic hybrid materials,[25,26] have been created through polymerization in the presence of the self-assembled BCPs.

Although BCPs contain high atomic carbon concentrations, ordered nanoporous carbon films have not been successfully fabricated through the direct pyrolysis of self-assembled BCPs.[27] This inability is attributed to the fact that linearly structured BCP compounds have very poor carbon yields in carbonization reactions. Furthermore, the survival of the nanostructures during high-temperature pyrolysis ($>800\,^{\circ}C$) is extremely challenging for the self-assembled BCP structures. This deficiency is associated with the linearly structured BCPs, which melt before carbonization reactions occur. The cross-linking of BCPs can significantly stabilize the self-assembled nanostructures. However, it is still difficult for the limited cross-linkage to preserve the preorganized nanostructures, because of the massive loss of carbon in the form of volatile carbon-containing species during pyrolysis.

Highly cross-linked resorcinol–formaldehyde resin (RFR) is a well-known carbonization source.[6,10] This rigid polymeric carbon precursor can retain the preorganized structures during pyrolysis. However, the low solubility of the highly cross-linked RFR in solvents makes it impossible to directly

[*] C. Liang, Dr. K. Hong, Dr. S. Dai
Chemical Sciences Division, Oak Ridge National Laboratory
Oak Ridge, TN 37831-6201 (USA)
Fax: (+1) 865-576-5235
E-mail: dais@ornl.gov
Prof. G. A. Guiochon, Prof. J. W. Mays
Department of Chemistry, The University of Tennessee
Knoxville, TN 37996-1600 (USA)

[**] This work was performed at the Oak Ridge National Laboratory and supported by the Office of Basic Energy Sciences, U.S. Department of Energy, under contract No. DE-AC05-00OR22725 with UT-Battelle, LLC. We thank Dr. A. C. Buchanan (ORNL) for helpful suggestions, and C.L. thanks TAML for the fellowship.

Supporting information for this article is available on the WWW under http://www.angewandte.org or from the author.

 DOI: 10.1002/ange.200461051

blend RFR with BCPs for the formation of nanostructured RFR. To overcome this limitation, we developed a stepwise assembly approach to fabricate highly ordered nanoporous carbon films. The essence of this methodology is to first preorganize the resorcinol monomers into a well-ordered nanostructured film with the assistance of polystyrene-*block*-poly(4-vinylpyridine) (PS-P4VP) self-assembly and solvent-induced structural annealing, which is followed by the in situ polymerization of the resorcinol monomers with formaldehyde vapor to form ordered nanostructured RFR. Upon carbonization, the nanostructured RFR is transformed into a highly ordered nanoporous carbon film with the concomitant decomposition of the PS-P4VP template to gaseous species. Figure 1 schematically illustrates the procedure for the

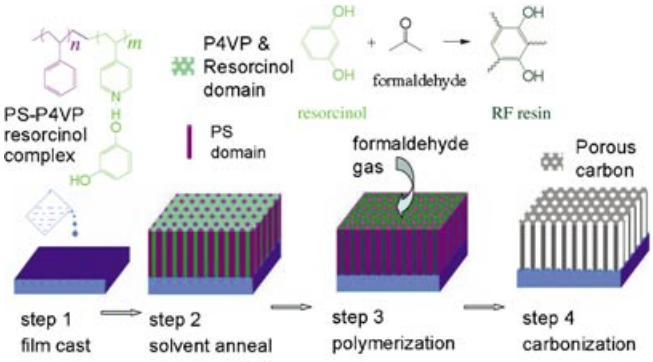

Figure 1. Schematic representation of the synthesis protocol used to prepare well-defined carbon nanostructures. Step 1: film casting of PS-P4VP/resorcinol supramolecular assembly. Step 2: completion of microphase separation by solvent annealing at 80 °C in DMF/benzene mixed vapor. The resorcinol is organized in the well-defined P4VP domain. Step 3: in situ polymerization of resorcinol and formaldehyde by exposing the film to formaldehyde gas. Highly cross-linked RFR is formed within the P4VP domain. Step 4: pyrolysis of the polymeric film in N_2. A hexagonal carbon-channel array is formed by sacrificing the block copolymer.

fabrication of ordered porous carbon films. The synthesis protocol involves four basic steps: 1) monomer–BCP film casting, 2) structure refining through solvent annealing, 3) polymerization of the carbon precursor, and 4) carbonization.

In step 1, the precursor films can be cast from a solution containing a mixture of PS-P4VP and resorcinol onto silica, silicon, glassy carbon, or copper, which can withstand the high temperature required by the final carbonization step. Both *N*,*N*′-dimethylformamide (DMF) and cyclohexanol are good solvents for PS-P4VP and can be used to cast the precursor films. The concentration of PS-P4VP is in the range of 0.5–10 wt %. The final film structures are not dependent on the casting method (dip coating or spin coating). The BCP template used in the synthesis has equal lengths of PS and P4VP blocks. The bulk material of this PS-P4VP copolymer has a lamellar structure.[15] The self-assembly of the PS-P4VP/resorcinol mixture is essentially driven by the hydrogen-bonding interaction between resorcinol and the P4VP block.[21,28] This strong hydrogen-bond association between the basic P4VP blocks and the acidic resorcinol monomers enriches the resorcinol molecules selectively in the P4VP domain. Accordingly, the volume fraction of the P4VP domain is significantly increased relative to that of the PS domain, resulting in a hexagonal structure.[15,21] The PS block in the PS-P4VP/resorcinol complex is the minor component, which forms cylindrical microdomains in the self-assembled film. Figure 2 compares the Fourier-transform infrared

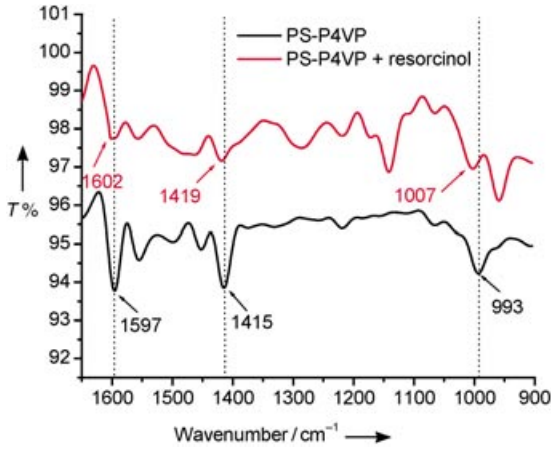

Figure 2. FTIR spectra of PS-P4VP and PS-P4VP/resorcinol mixture in the region from 900 to 1650 cm^{-1}. The characteristic peaks of the pyridine ring in PS-P4PVP at 993, 1415, and 1597 cm^{-1} shift to 1007, 1419, and 1602 cm^{-1}, respectively, as a result of the hydrogen-bonding interaction with resorcinol. *T* = transmittance.

(FTIR) spectrum of PS-P4VP and that of the PS-P4VP/resorcinol mixture (molar ratio of pyridine groups to resorcinol 1:1). The characteristic stretching modes of the P4VP block at 993, 1415, and 1597 cm^{-1} shift to 1007, 1419, and 1602 cm^{-1}, respectively, for the PS-P4VP/resorcinol mixture. These vibrational frequency shifts are consistent with a hydrogen-bonding interaction between the pyridine groups and the resorcinol molecules.[28]

The second step involves solvent annealing,[21,29] which is the key to the formation of highly ordered and well-oriented nanostructures. Russell and co-workers reported an efficient method based on solvent annealing for refining self-assembled block copolymer nanostructures.[29] The controlled evaporation of the solvent results in highly ordered nanostructures oriented normal to the substrate. The as-cast film is annealed in DMF/benzene vapor at 80 °C through a slow evaporation of the solvents over a period of 24 h, to give a final carbon film having a highly ordered hexagonal structure with all pores oriented perpendicular to the substrate. DMF is a highly miscible solvent for the PS and P4VP blocks, and both blocks have quite good mobility when the film is swollen in DMF vapor. As a result of this mobility, the swollen PS and P4VP blocks repel one another and tend to organize into a well-defined structure.[29] However, the repulsion of these two blocks is damped by DMF, which is highly miscible with both blocks. We found that the addition of benzene vapor greatly accelerates the self-assembly process and significantly enhances the order of the film.[29] Benzene is a good solvent only for the PS block, so the absorbed benzene vapor is most likely enriched in the PS block domain. Therefore, the repulsion

between the PS and P4VP domains is enhanced by benzene. A fast microphase separation is thus achieved in the DMF/benzene mixed vapor.

In step 3, the solvent-annealed nanostructured film was exposed to formaldehyde vapor to cross-link the resorcinol molecules into a highly cross-linked phenolic resin located in the P4VP domain. The cross-linking was carried out by vapor/solid reactions with minimum perturbation of the self-assembled nanostructures. The reaction rate can be readily controlled by the vapor pressure of formaldehyde.

The final step involves the decomposition of the BCP template to generate ordered nanopores, and the carbonization of the nanostructured RFR to form the carbon pore walls. This pyrolysis process was studied by using thermogravimetric analysis (TGA) to continuously measure the mass loss upon heating from room temperature to 800 °C under argon at 20 °C min^{-1}. Figure 3 shows the thermograms (TGs)

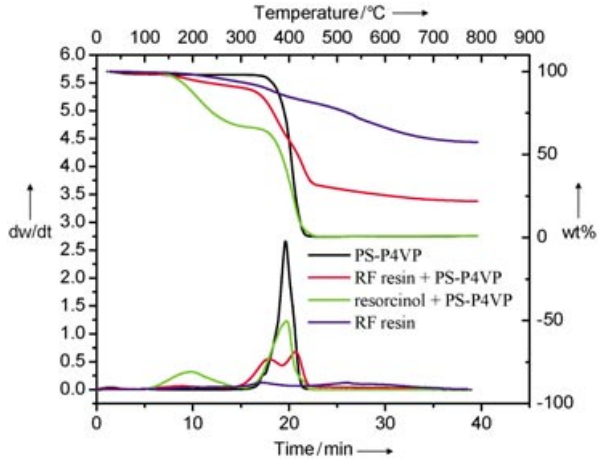

Figure 3. TGA and dTG curves for PS-*block*-P4VP (black), PS-*block*-P4VP/resorcinol mixture (molar ratio of pyridine groups to resorcinol 1:1) (green), resorcinol–formaldehyde resin (RFR) (blue), and PS-*block*-P4VP plus RFR (red). The top and right-hand axes are the temperature and wt% for the thermogram (TG). The left-hand and bottom axes show the weight loss rate and time for the derivative thermogram (dTG).

and the derivative thermograms (dTGs) of four samples: PS-P4VP, PS-P4VP/resorcinol mixture, RFR, and PS-P4VP plus RFR. The pure PS-P4VP sample starts to decompose at 328 °C and finishes at 430 °C with only negligible residue (0.7 wt %). Both the decomposition temperature and the reaction rate of the PS and P4VP blocks are too close to be resolved in the TG and dTG curves. Therefore, the pyrolysis of PS-P4VP exhibits only one peak in the dTG curve of the pure PS-P4VP sample. The TG curve of the PS-P4VP/resorcinol mixture has two weight-loss stages with corresponding dTG peaks at 195 and 392 °C. The weight loss for the first stage starts at 120 °C, which is only 10 °C above the melting point of resorcinol. The first weight-loss stage ends at 284 °C with the loss of about 34 wt %. The mixture of PS-P4VP and resorcinol has 33.87 wt % of resorcinol. Accordingly, this weight loss in the TG curve indicates that all the resorcinol molecules evaporated before the temperature reached 284 °C. The second weight-loss stage of the PS-P4VP/resorcinol mixture starts at 328 °C and ends at 430 °C. This part of the weight loss is attributed to the decomposition of the PS-P4VP copolymer. The TGA curve of the RFR sample exhibits a continuous weight loss from 200 to 750 °C. The carbonization yield for pyrolysis of RFR is 57.59 wt %. The TGA curve of the PS-*block*-P4VP and RFR sample, prepared by cross-linking the PS-P4VP/resorcinol mixture using formaldehyde vapor, shows a complex pyrolysis behavior. A significant weight loss was found in the range of 200 to 750 °C. The major weight loss occurs from 320 to 430 °C, which is attributed to the decomposition of the PS-P4VP copolymer. The two dTG peaks emerge in this zone, which indicates two different types of decomposition behavior. Comparison of these peaks with the dTG peak of the pure PS-P4VP suggests that the RFR affects the pyrolysis of the PS-P4VP. The decomposition of the PS domain is the least affected, as the RFR is localized in the P4VP domain. The P4VP chain is tangled with the RFR; as a result, the decomposition rate of P4VP may be retarded by RFR because of the interaction between RFR and P4VP. Therefore, the P4VP block may decompose after the PS block. The pyrolysis of the PS-P4VP/RFR mixture yields 22.16 % carbon at 800 °C. After taking into account the weight gain in the polymerization with formaldehyde, the weight percentage of the RFR in the PS-P4VP/RFR mixture rises from 33.87 % (resorcinol wt % in PS-P4VP/resorcinol mixture) to 37.34 %. If one assumes that RFR in the P4VP domain has the same carbon yields as the pure RFR (57.59 %), the PS-P4VP part only accounts for 1.05 wt % carbon in the final product. Clearly, the RFR is the predominant carbon source of the porous carbon film and the BCP is sacrificed as pores.

A crack-free nanoporous carbon film with thickness from several tens of nanometers up to ~1 μm and size up to 6 cm^2 can be obtained. The nanoporous carbon film strongly adheres to substrates and is homogeneous in thickness. The nanopores are oriented perpendicular to the film surface (Figure 4 a, d). An enlarged Z-contrast image of the carbon film is shown in Figure 4 b. The Fourier transform of this Z-contrast image of the film shows a pattern of multiple reflections, which confirms that the film has a highly ordered hexagonal-pore array. Based on Figure 4 c, the pore diameter is 33.7 ± 2.5 nm and the wall thickness is 9.0 ± 1.1 nm. The volume fraction of the straight channels is about 0.565 (see Supporting Information for details). The pore diameter and thickness can be controlled by the volume fractions of PS in BCP and carbon-forming resin, respectively. The cross section of the film scratched from a film substrate is shown in Figure 4 d. All straight channels are across the whole film. The inset in the lower right-hand corner is the Fourier transform of the high-resolution scanning electron microscopy (SEM) image of the film cross section, which reflects parallel periodical channels. No graphitic structure was found in the high-resolution transmission electron microscopy (HRTEM) mode, which suggests that the wall is amorphous carbon. Wide-angle X-ray diffraction (WAXD) shows broad peaks at 23.6, 43.76, and 80.24°, which are characteristic of amorphous carbon. The Raman spectrum shows a broad D band at 1333 cm^{-1}, which overlaps with the G band at 1600 cm^{-1}. Such

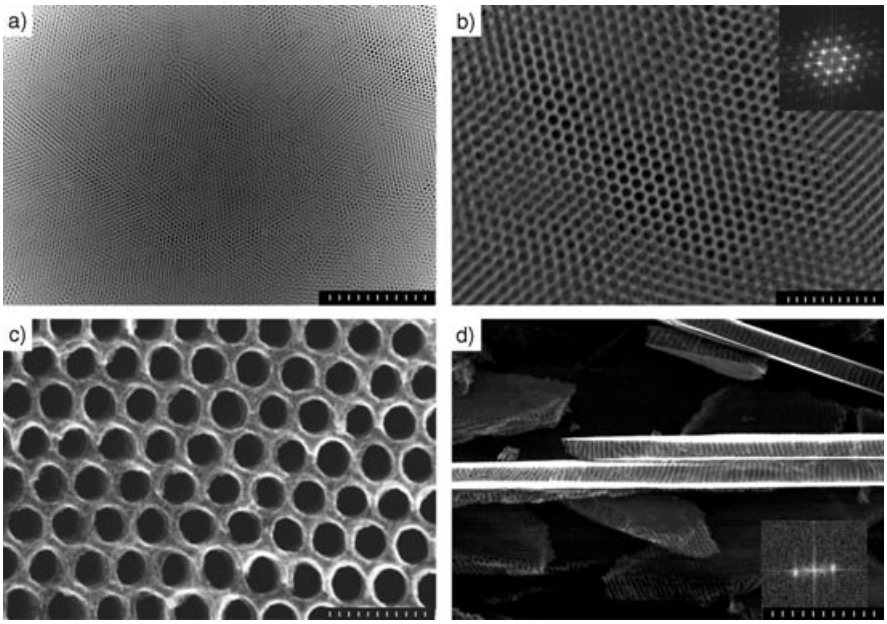

Figure 4. Electron microscopy images of the carbon film. a) Z-contrast image of the large-scale homogeneous carbon film in a 4×3 μm area. The scale bar is 1 μm. b) Z-contrast image showing details of the highly ordered carbon structure. In the inset, a Fourier transform (FT) of the image shows a pattern with multiple reflections, which are characteristic of a highly ordered hexagonal array. The scale bar is 300 nm. c) High-resolution SEM image of the surface of the carbon film with uniform hexagonal-pore array. The pore size is 33.7 ± 2.5 nm and the wall thickness is 9.0 ± 1.1 nm. The scale bar is 100 nm. d) SEM image of the film cross section, which exhibits all parallel straight channels perpendicular to the film surface. The scale bar is 100 nm. The inset is the FT of the cross section image. The FT pattern shows the reflections of the periodic parallel channels.

a broad D band is reminiscent of the glassy carbon texture. The HRTEM image, WAXD pattern, and Raman spectrum are included in the Supporting Information.

In conclusion, a facile methodology based on stepwise self-assembly has been successfully developed to prepare highly ordered and well-oriented mesoporous carbon films through carbonization of a nanostructured phenolic resin and BCP composite. The BCPs play two important roles in the synthesis: 1) directing the formation of the phenolic resin nanostructure and 2) serving as templates for nanopores. The orientation of the ordered carbon nanopores was successfully aligned normal to the substrates using a solvent annealing process. The unique structural feature of this oriented nanoporous carbon film highlights opportunities in areas such as separation membranes, chemical sensors, and catalysts.

Experimental Section

PS-P4VP (0.1 g)—with number average molecular masses (M_n) of 11800 g mol^{-1} for PS and 11500 g mol^{-1} for P4VP, and M_w/M_n of 1.04 for both blocks—and resorcinol (0.0512 g) were dissolved in DMF (2 g). This solution was heated at 100 °C for 4 h to ensure the formation of hydrogen bonds. After cooling to room temperature, a drop of solution was cast into a film on a silica plate by spin coating at 1000 rpm for 2 min. The film was dried in a hood, then placed in a preheated chamber at 80 °C along with two small vials which contained DMF and benzene. The film was kept in the sealed chamber for 24 h to allow the completion of microphase separation by a slow evaporation of the solvents. The microphase-separated film was sequentially cured by exposure to formaldehyde gas at 100 °C for 4 h. The cured film was finally carbonized in nitrogen using a temperature ramp of 1 °C min^{-1} to 800 °C.

Received: June 23, 2004

Keywords: block copolymers · carbon · mesoporous materials · nanostructures · self-assembly

[1] T. Rueckes, K. Kim, E. Joselevich, G. Y. Tseng, C. L. Cheung, C. M. Lieber, *Science* **2000**, *289*, 94 – 97.
[2] L. S. Schadler, S. C. Giannaris, P. M. Ajayan, *Appl. Phys. Lett.* **1998**, 73, 3842 – 3844.
[3] a) M. B. Shiflett, H. C. Foley, *Science* **1999**, 285, 1902 – 1905; b) J. Pang, X. Li, D. Wang, Z. Wu, V. T. John, Z. Yang, Y. F. Lu, *Adv. Mater.* **2004**, *16*, 884 – 886.
[4] B. J. Hinds, N. Chopra, T. Rantell, R. Andrews, V. Gavalas, L. G. Bachas, *Science* **2004**, *303*, 62 – 65.
[5] S. A. Miller, V. Y. Young, C. R. Martin, *J. Am. Chem. Soc.* **2001**, *123*, 12335 – 12342.
[6] C. D. Liang, S. Dai, G. A. Guiochon, *Anal. Chem.* **2003**, *75*, 4904 – 4912.
[7] S. H. Joo, S. J. Choi, I. Oh, J. Kwak, Z. Liu, O. Terasaki, R. Ryoo, *Nature* **2001**, *412*, 169 – 172.
[8] A. C. Dillon, K. M. Jones, T. A. Bekkedahl, C. H. Kiang, D. S. Bethune, M. J. Heben, *Nature* **1997**, *386*, 377 – 379.
[9] H. J. Dai, J. H. Hafner, A. G. Rinzler, D. T. Colbert, R. E. Smalley, *Nature* **1996**, *384*, 147 – 150.
[10] A. A. Zakhidov, R. H. Baughman, Z. Iqbal, C. X. Cui, I. Khayrullin, S. O. Dantas, I. Marti, V. G. Ralchenko, *Science* **1998**, *282*, 897 – 901.
[11] K. H. Kwok, W. K. S. Chiu, *Carbon* **2003**, *41*, 673 – 680.
[12] Y. G. Gogotsi, M. Yoshimura, *Nature* **1994**, *367*, 628 – 630.
[13] A. Singh, J. Jayaram, M. Madou, S. Akbar, *J. Electrochem. Soc.* **2002**, *149*, E78-E83.
[14] E. Huang, L. Rockford, T. P. Russell, C. J. Hawker, *Nature* **1998**, *395*, 757 – 758.
[15] S. Jain, F. S. Bates, *Science* **2003**, *300*, 460 – 464.
[16] M. Park, C. Harrison, P. M. Chaikin, R. A. Register, D. H. Adamson, *Science* **1997**, *276*, 1401 – 1404.
[17] J. Ruokolainen, R. Makinen, M. Torkkeli, T. Makela, R. Serimaa, G. ten Brinke, O. Ikkala, *Science* **1998**, *280*, 557 – 560.
[18] R. T. Clay, R. E. Cohen, *Supramol. Sci.* **1998**, *5*, 41 – 48.
[19] M. Antonietti, E. Wenz, L. Bronstein, M. Seregina, *Adv. Mater.* **1995**, *7*, 1000.
[20] R. A. Pai, R. Humayun, M. T. Schulberg, A. Sengupta, J. N. Sun, J. J. Watkins, *Science* **2004**, *303*, 507 – 510.
[21] A. Sidorenko, I. Tokarev, S. Minko, M. Stamm, *J. Am. Chem. Soc.* **2003**, *125*, 12211 – 12216.
[22] U. Y. Jeong, D. Y. Ryu, J. K. Kim, D. H. Kim, T. P. Russell, C. J. Hawker, *Adv. Mater.* **2003**, *15*, 1247 – 1250.
[23] D. Y. Zhao , J. L. Feng, Q. S. Huo, N. Melosh, G. H. Fredrickson, B. F. Chmelka, G. D. Stucky, *Science* **1998**, *279*, 548 – 552.
[24] X. Feng, G. E. Fryxell, L. Q. Wang, A. Y. Kim, J. Liu, K. M. Kemner, *Science* **1997**, *276*, 923 – 926.
[25] Z. T. Zhang, S. Dai, *J. Am. Chem. Soc.* **2001**, *123*, 9204 – 9205.

[26] Y. F. Lu, Y. Yang, A. Sellinger, M. C. Lu, J. M. Huang, H. Y. Fan, R. Haddad, G. Lopez, A. R. Burns, D. Y. Sasaki, J. Shelnutt, C. J. Brinker, *Nature* **2001**, *410*, 913 – 917.
[27] T. Kowalewski, N. V. Tsarevsky, K. Matyjaszewski, *J. Am. Chem. Soc.* **2002**, *124*, 10632 – 10633.
[28] O. T. Ikkala, J. Ruokolainen, G. ten Brinke, M. Torkkeli, R. Serimaa, *Macromolecules* **1995**, *28*, 7088 – 7094.
[29] S. H. Kim, M. J. Misner, T. Xu, M. Kimura, T. P. Russell, *Adv. Mater.* **2004**, *16*, 226 – 231.

